

Structurally Distinct Cation Channelrhodopsins from Cryptophyte Algae

Elena G. Govorunova,¹ Oleg A. Sineshchekov,¹ and John L. Spudich^{1,*}

¹Center for Membrane Biology and Department of Biochemistry and Molecular Biology, University of Texas Health Science Center at Houston, McGovern Medical School, Houston, Texas

ABSTRACT Microbial rhodopsins are remarkable for the diversity of their functional mechanisms based on the same protein scaffold. A class of rhodopsins from cryptophyte algae show close sequence homology with haloarchaeal rhodopsin proton pumps rather than with previously known channelrhodopsins from chlorophyte (green) algae. In particular, both aspartate residues that occupy the positions of the chromophore Schiff base proton acceptor and donor, a hallmark of rhodopsin proton pumps, are conserved in these cryptophyte proteins. We expressed the corresponding polynucleotides in human embryonic kidney (HEK293) cells and studied electrogenic properties of the encoded proteins with whole-cell patch-clamp recording. Despite their lack of residues characteristic of the chlorophyte cation channels, these proteins are cation-conducting channelrhodopsins that carry out light-gated passive transport of Na^+ and H^+ . These findings show that channel function in rhodopsins has evolved via multiple routes.

Phototaxis receptors that depolarize the membranes of green (chlorophyte) algae (1) act as light-gated cation channels when expressed in animal cells (2,3). This unique property earned them the name “channelrhodopsins” and made them molecules of choice for optogenetic depolarization of the cell membrane and neuronal activation (4). In the phylogenetically distant cryptophyte algae, another family of channelrhodopsins with strictly anion selectivity was found and used to hyperpolarize the membrane and neuronal inhibition (5). Although these latter proteins, called anion channelrhodopsins, share some sequence homology with cation channelrhodopsins (CCRs) from green algae, their conduction mechanisms are clearly different (6–8).

Guillardia theta, the only cryptophyte organism the genome of which has been completely sequenced (9), is predicted to encode at least 53 microbial (type 1) rhodopsins (5). Except for the anion channelrhodopsins, few other rhodopsins from this organism have been investigated by heterologous expression (10). One cluster of *G. theta* rhodopsin protein models contains nine sequences, the closest homologs of which, besides similar proteins from other cryptophytes and uncharacterized fungal proteins, are haloarchaeal rhodopsins (Fig. S1 in the Supporting Material). Here we show that these proteins (which we

designate as cryptophyte CCRs) are light-gated cation channels with distinctly different structures than those of previously known chlorophyte CCRs from green algae.

We synthesized human codon-adapted versions of three polynucleotides corresponding to the *G. theta* predicted transcripts 99928 (GenBank: KU761992), 120390 (GenBank: KU761994) and 162755 (GenBank: KU761993). The encoded polypeptides extend 150–200 residues beyond the seven-transmembrane-helix (rhodopsin) domain, but no other putative domains could be detected. We also included in our analysis a highly homologous protein from the cryptophyte alga *Proteomonas sulcata* (GenBank: KF992056) previously shown to generate photocurrents in neurons (11). We also synthesized a construct (GenBank: KU761991) corresponding to *G. theta* model 135937, but it was nonfunctional in our system.

An alignment of the rhodopsin domains showed a closer match of cryptophyte CCRs with haloarchaeal proton pumps than with chlorophyte CCRs (Fig. S2). Asp residues in the positions of the retinylidene Schiff base proton acceptor and donor (Asp-85 and Asp-96 in *Halobacterium salinarum* bactiorhodopsin (*HsBR*), respectively) are conserved in all four studied cryptophyte CCRs, whereas in the majority of chlorophyte CCRs Asp-85 is replaced with Glu, and Asp-96, with His (Fig. 1). Proton transport activity was not observed in a previously studied rhodopsin from the same organism, *GtR1*, which also has Asp residues in both proton acceptor and donor positions, and a rhodopsin from the fungus *Neurospora*, NR, in which Asp-85 is conserved and Asp-96 is found as Glu (10,12).

Submitted March 15, 2016, and accepted for publication May 2, 2016.

*Correspondence: john.l.spudich@uth.tmc.edu

Editor: Andreas Engel.

<http://dx.doi.org/10.1016/j.bpj.2016.05.001>

© 2016 Biophysical Society.

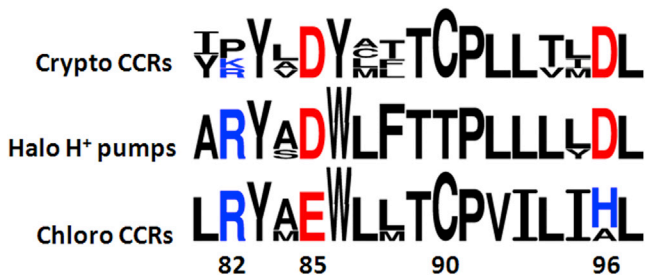


FIGURE 1 Sequence logos of the transmembrane helix 3 generated with WebLogo 3 (17) from the alignment shown in Fig. S2. The numbering is according to the *HsBR* sequence.

None of the five conserved Glu residues in helix 2 of chlorophyte CCRs (highlighted green in Fig. S2) that contribute to their cation translocation pathway (13) is conserved in the tested cryptophyte proteins. However, cryptophyte CCRs share with CCRs from green algae a Cys residue in the position of Thr-90 in *HsBR* (Fig. 1). Arg-82 (*HsBR* numbering), conserved in most microbial rhodopsins, is replaced with Pro or Lys in *G. theta* CCRs. Modification of the Arg-82 homolog in an H^+ -pumping rhodopsin from the green alga *Coccomyxa* converted it into an operational H^+ channel (14).

We expressed the constructs encoding the rhodopsin domains of four cryptophyte CCRs fused to enhanced yellow fluorescent protein in human embryonic kidney (HEK293) cells and tested their electrogenic function with whole-cell patch-clamp. Under our standard conditions (the holding potential (E_h) -60 mV, 150 mM NaCl in the bath, 126 mM KCl in the pipette, pH 7.4; for other details, see the Supporting Material), all four proteins generated inward currents in response to a light pulse. The mean amplitudes and half-decay rates of the photocurrents are shown in Fig. S3. Protein 99928 generated the largest currents,

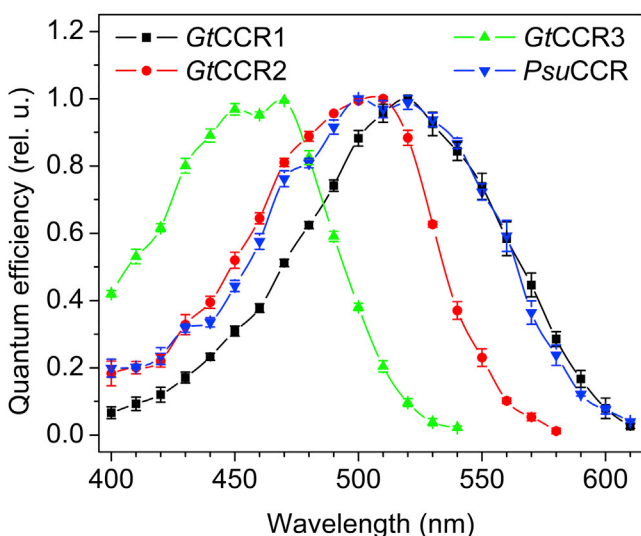


FIGURE 2 The action spectra of photocurrents generated by cryptophyte CCRs in HEK293 cells.

whereas the currents from the other three proteins were considerably smaller.

The action spectra of the photocurrents are shown in Fig. 2. In the genomes of most green algae, only two channelrhodopsin homologs have been found. According to a historical convention, the more red-shifted rhodopsin from the same organism is assigned the number 1, and the more blue-shifted is assigned the number 2 (1).

As shown below, all three *G. theta* rhodopsins tested in this study are nonselective light-gated cation channels. Therefore, we assigned the abbreviation *GtCCR1* to the most red-shifted one (120390) with the maximal sensitivity at 520 nm; *GtCCR2*, to the more blue-shifted rhodopsin (99928) with

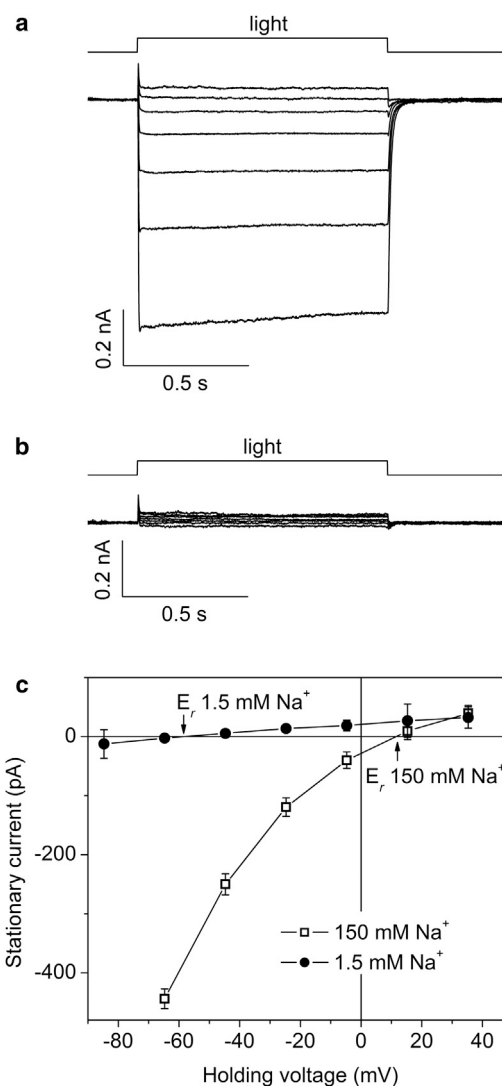


FIGURE 3 Representative series of photocurrents generated by *GtCCR2* in a HEK293 cell at 150 (a) and 1.5 (b) mM Na^+ in the bath. E_h was changed in 20 -mV steps from -80 to 40 mV at the amplifier output (bottom to top). (c) The current-voltage relationship for the cell shown in (a) and (b). The data are the mean values mean \pm SE ($n = 3$) corrected for liquid junction potentials.

the peak at 505 nm; and *GtCCR3*, to the most blue-shifted rhodopsin (162755) with peaks at ~460 nm. The spectral maximum of this latter protein corresponds to that of the *G. theta* photoaccumulation response (10).

Initially, when no information regarding its ionic selectivity was available, the homologous protein from *P. sulcata* was referred to as “*PsChR2*” (11). To avoid confusion with CCRs from the chlorophyte alga *Platymonas subcordiformis* (15), we will call it *PsuCCR* in this study. No number can be assigned to this rhodopsin as yet, because the spectral properties of its several other homologs from the same organism (Fig. S1) have not yet been determined.

Upon shifting E_h to more positive values, the photocurrents generated by cryptophyte CCRs reversed their direction (Fig. 3 a). The current-voltage dependencies (IE curves) measured under standard conditions exhibited a significant inward rectification (Fig. 3 c, open squares).

To identify the nature of the transported ions, we determined reversal potentials (E_r) upon variation of the ionic composition of the bath solution. When Na^+ concentration in the bath was reduced 100-fold by partial replacement with *n*-methyl-D-glucamine (NMG^+), a dramatic inhibition of photocurrents was observed (Fig. 3 b). Moreover, for all tested proteins, E_r shifted to more negative values (Figs. 3 c, solid circles, and S4), indicating that they passively transported Na^+ across the cell membrane.

A 100-fold reduction of the bath H^+ concentration (from pH 5.4 to pH 7.4) also led to an E_r shift to negative values, although its magnitude was smaller than that for Na^+ (Fig. S4). Therefore, we concluded that cryptophyte CCRs transport both Na^+ and H^+ , as do chlorophyte CCRs from green algae. Purely passive H^+ influx has also been demonstrated at low extracellular pH and negative membrane potentials for some rhodopsin H^+ pumps, such as that from *Gloeobacter violaceus* (16) i.e., a leaky-pump phenomenon. However, channel currents generated by cryptophyte CCRs cannot be explained by this mechanism, because at physiological conditions they are carried practically only by Na^+ ions (Fig. 3). Na^+ pumping can be excluded, because the direction of photocurrents depended on the Nernst equilibrium potential for Na^+ .

Our results indicate that the microbial rhodopsin common ancestor of chlorophyte and cryptophyte CCRs converged on the same function through structurally different paths. Further research is needed to elucidate the mechanisms of cation conductance in cryptophyte CCRs, but it is already clear that their identification expands our current concepts about channelrhodopsins in an unexpected direction.

SUPPORTING MATERIAL

Four figures are available at [http://www.biophysj.org/biophysj/supplemental/S0006-3495\(16\)30274-0](http://www.biophysj.org/biophysj/supplemental/S0006-3495(16)30274-0).

ACKNOWLEDGMENTS

This work was supported by National Institutes of Health grants No. R01GM027750 and No. U01MH109146 and Endowed Chair No. AU-0009 from the Robert A. Welch Foundation.

REFERENCES

1. Sineshchekov, O. A., K.-H. Jung, and J. L. Spudich. 2002. Two rhodopsins mediate phototaxis to low- and high-intensity light in *Chlamydomonas reinhardtii*. *Proc. Natl. Acad. Sci. USA*. 99:8689–8694.
2. Nagel, G., D. Ollig, ..., P. Hegemann. 2002. Channelrhodopsin-1: a light-gated proton channel in green algae. *Science*. 296:2395–2398.
3. Nagel, G., T. Szellas, ..., E. Bamberg. 2003. Channelrhodopsin-2, a directly light-gated cation-selective membrane channel. *Proc. Natl. Acad. Sci. USA*. 100:13940–13945.
4. Boyden, E. S., F. Zhang, ..., K. Deisseroth. 2005. Millisecond-time-scale, genetically targeted optical control of neural activity. *Nat. Neurosci.* 8:1263–1268.
5. Govorunova, E. G., O. A. Sineshchekov, ..., J. L. Spudich. 2015. NEUROSCIENCE. Natural light-gated anion channels: A family of microbial rhodopsins for advanced optogenetics. *Science*. 349:647–650.
6. Sineshchekov, O. A., E. G. Govorunova, ..., J. L. Spudich. 2015. Gating mechanisms of a natural anion channelrhodopsin. *Proc. Natl. Acad. Sci. USA*. 112:14236–14241.
7. Govorunova, E. G., O. A. Sineshchekov, and J. L. Spudich. 2015. *Proteomonas sulcata* ACR1: a fast anion channelrhodopsin. *Photochem. Photobiol.* 92:257–263.
8. Sineshchekov, O. A., H. Li, ..., J. L. Spudich. 2016. Photochemical reaction cycle transitions during anion channelrhodopsin gating. *Proc. Natl. Acad. Sci. USA*. 201525269.
9. Curtis, B. A., G. Tanifugi, ..., J. M. Archibald. 2012. Algal genomes reveal evolutionary mosaicism and the fate of nucleomorphs. *Nature*. 492:59–65.
10. Sineshchekov, O. A., E. G. Govorunova, ..., J. L. Spudich. 2005. Rhodopsin-mediated photoreception in cryptophyte flagellates. *Bioophys. J.* 89:4310–4319.
11. Klapoetke, N. C., Y. Murata, ..., E. S. Boyden. 2014. Independent optical excitation of distinct neural populations. *Nat. Methods*. 11:338–346.
12. Brown, L. S., A. K. Dioumaev, ..., J. L. Spudich. 2001. Photochemical reaction cycle and proton transfers in *Neurospora* rhodopsin. *J. Biol. Chem.* 276:32495–32505.
13. Kato, H. E., F. Zhang, ..., O. Nureki. 2012. Crystal structure of the channelrhodopsin light-gated cation channel. *Nature*. 482:369–374.
14. Vogt, A., Y. Guo, ..., P. Hegemann. 2015. Conversion of a light-driven proton pump into a light-gated ion channel. *Sci. Rep.* 5:16450.
15. Govorunova, E. G., O. A. Sineshchekov, ..., J. L. Spudich. 2013. Characterization of a highly efficient blue-shifted channelrhodopsin from the marine alga *Platymonas subcordiformis*. *J. Biol. Chem.* 288:29911–29922.
16. Vogt, A., J. Wietek, and P. Hegemann. 2013. *Gloeobacter* rhodopsin, limitation of proton pumping at high electrochemical load. *Biophys. J.* 105:2055–2063.
17. Crooks, G. E., G. Hon, ..., S. E. Brenner. 2004. WebLogo: a sequence logo generator. *Genome Res.* 14:1188–1190.

Supplemental Information

**Structurally Distinct Cation Channelrhodopsins from Cryptophyte
Algae**

Elena G. Govorunova, Oleg A. Sineshchekov, and John L. Spudich

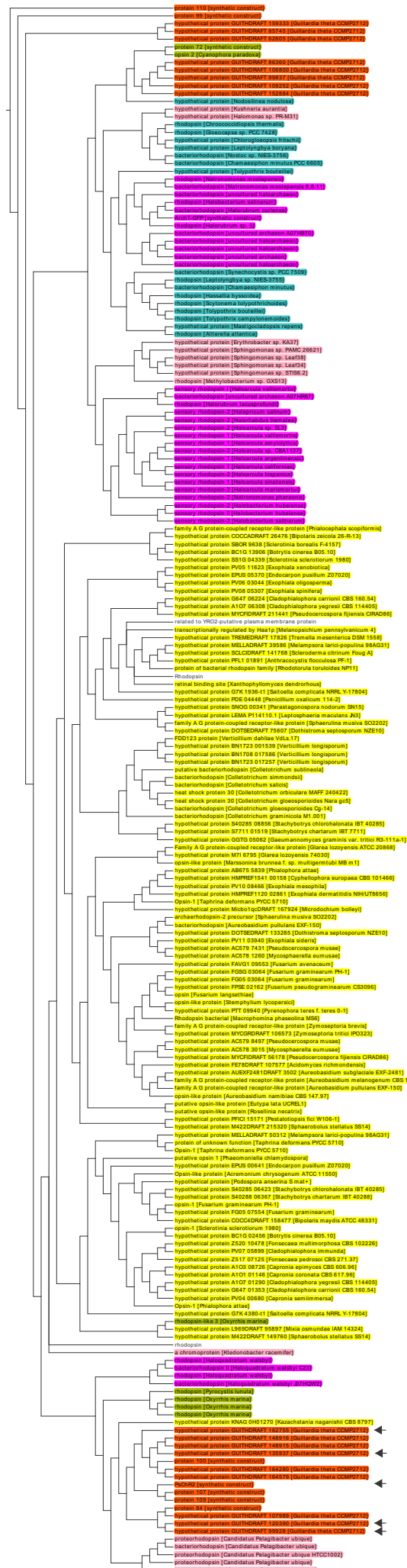
Supporting Material

Structurally distinct cation channelrhodopsins from cryptophyte algae

Elena G. Govorunova, Oleg A. Sineshchekov, and John L. Spudich

Center for Membrane Biology, Department of Biochemistry and Molecular Biology, University of Texas Health Science Center at Houston
McGovern Medical School, Houston, Texas, USA

Address reprint requests and inquiries to John.L.Spudich@uth.tmc.edu



Supporting figure 1. A phylogenetic tree of 500 closest homologs of the rhodopsin domain of *Guillardia theta* protein model 99928 found in the NCBI non-redundant translated nucleotide database by Position-Specific Iterated BLAST. The hits are color-coded according to the phylogenetic position of their source organisms: orange, cryptophytes; yellow, fungi; olive, other eukaryotes; magenta, haloarchaea; cyan, cyanobacteria; pink, other prokaryotes; not colored, microbial rhodopsins from undefined source organisms. Proteins tested in this study are marked with the black arrows on the right. Some redundant entries have been manually removed by the Dendroscope 3 software (1). The tree was visualized using the EvolView server (2).

helix 1**helix 2**

GtCCR1	: IAANWISFLVIAGSFVVLCFISLRYKGPGGNENYY-----	NGFREQNMLTVIINLWCALAYFAKVLQSHSDDDGFVP-----	: 79
GtCCR2	: ITANWISFLAISASFIIILVISLRYKGPGGTESFY-----	NGFKEQNMLTVFINLWCALAYFAKVLQSHSNDNGFAP-----	: 79
GtCCR3	: IAADWIGFIAFGSSLAVALYKLVTFKGPDQDDVYF-----	FGYREEKMISVFVNLFAAALAYWAKLASHANGDVGPAAS-----	: 91
PsuCCR	: IIAHWTFFFHMITTFLGYVSFHSKGPGGKQPYF-----	AGYHEENNIGIFVNLFAAISYFGKVVSNDTHGHNYQNVGPFII	: 102
HsBR	: QITGRPEWIWLALGTALMGLTLYFLVKGMGVSD-----	PDAKKFYAITTLVPAIAFTMYLSMLLGYGLTMVPFG--GEQNP	: 77
HspAR2	: LNDGRPETLWLIGITLLMLIGTFYFIARGWGVT-----	KEAREYYAITILVPGIASAAYLAMFFGIGVTEVELAS-GTVLD	: 88
HsoAR3	: LGDGRPETLWLIGITLLMLIGTFYFLVRGVGVT-----	KDAREYYAVTILVPGIASAAYLAMFFGIGLTVTVEG--GEMLD	: 87
HaCR1	: MPEPGSEAIWLWLGTAGMFLGMLYFIARGWGETD-----	SRRQKFYIATILITAIAFVNVLAMALGFGLTIVEFA--GEEHP	: 78
CrChR1	: GSVICIPNNQCFCLAWLKSGNTNAEKLAAANILQWITFALSALCLMFYGYQTWKSTCGWEIYVATIEMIKFIEYFHEFDEPAVIYSSNGNK		: 154
CrChR2	: VNGSVLVPEDQCYCAGWIESRGTNQTAQTSNVLQWLAAGFSILLMFYAYQTWKSTCGWEIYVCAIEMVKVILEFFFEEFKNPSMLYLATGHR		: 115
PsChR2	: NPEYLNSETILDDCTPIYLNVGPLWEQKVARGTQWFGVILSLAFLIYYIWITYKATCGWEELYVCTIEFKKIVIELYFEFSPPAMIVQTNGEV		: 98
MvChR1	: IRYFVENDFEGCIPGHFDQYSSHGSLHDIVKAALYICMVISILQILFYGFQWWRKTCGWVWFVACIETSIYIIAITSEADSPFTLYLTNGQI		: 134

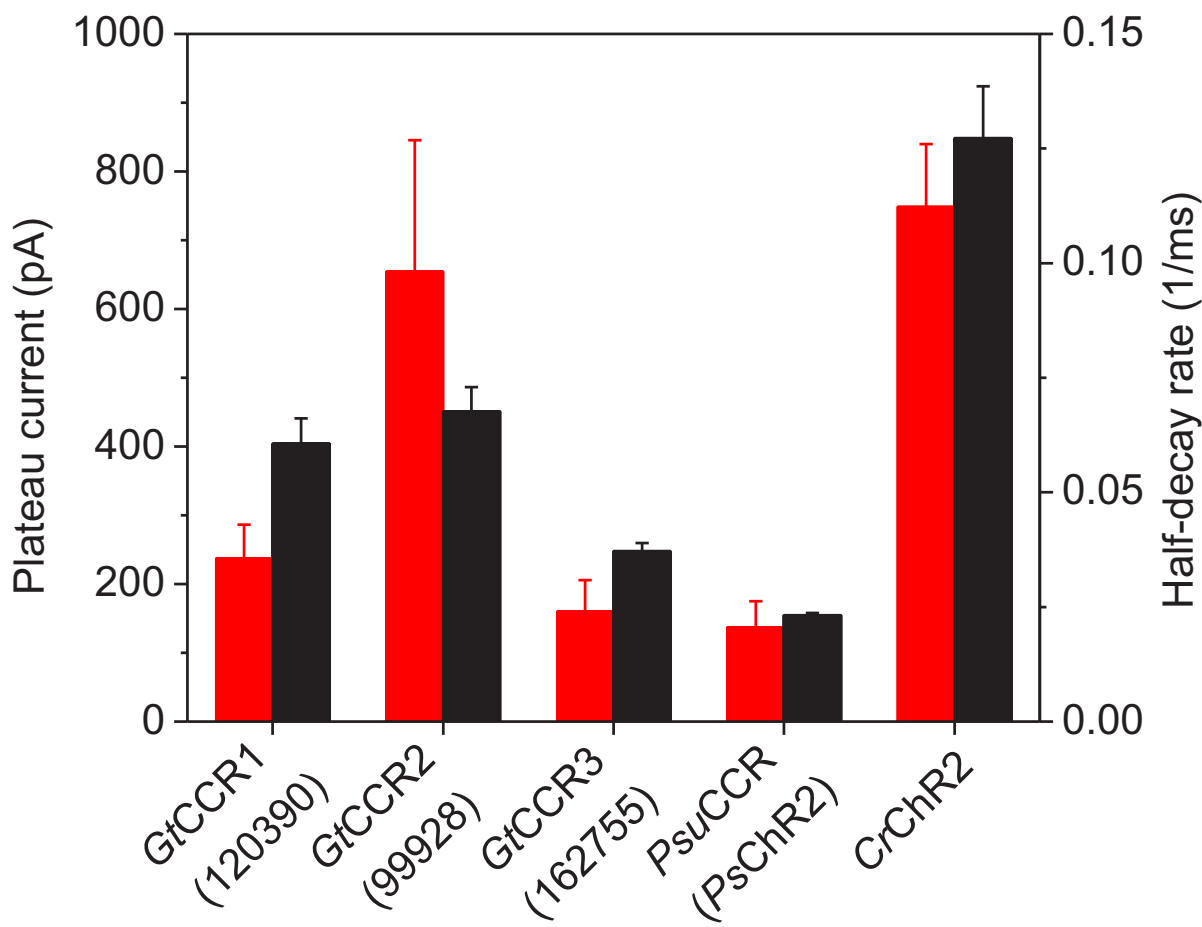
helix 3**helix 4****helix 5**

GtCCR1	: LTKIPYLDYATTCPPLTLDDMWCLDAPYKITSAVLVFTVMITGVACSLAVAP---	YSFYWFAMGMVLFIFTYVLMISIVRERLEFITQCAHD	: 168
GtCCR2	: LTVIPYVDYCTTCPPLTLDDILWCLDAPYKISSAVLVFTCLVIAVACSLAVAP---	FSYCWFMGMVLFIFTYVFLSIVRQLDFFTLCARD	: 168
GtCCR3	: VTTYKYLDYLTCPPLTIDILWLCLNLPYKFTFGAIVAVCILCAFMASVIPP-----	ARYMWFGMGITVESAASFNLKLRMRMLEQFVSKEA-	: 178
PsuCCR	: LGNYRYADYMLTCPPLLMDLLFQLRAPYKITCAMLIFAVLMI	GAVTNFYPGDDMKGPAAWFCFGFWYLIAYIFMAHIVSKQYGRLDYLAHG	: 195
HsBR	: IYWARYADWLFTTPPLLLDIALLVDADQGTILALVGADGIMIGTGLVGALT-----	KVSYRFVWWAISTAAMLYIYVLFVFFGFTSKAES	: 162
HspAR2	: IYYARYADWLFTTPPLLLDIALLAKVDRVTIGTLIGVDALMIVTGLIGALS-----	KTPLARYTWWLFSTIAFLFVYVYLLTSLRSAAK	: 173
HsoAR3	: IYYARYADWLFTTPPLLLDIALLAKVDRVTIGTLGVVDALMIVTGLIGALS-----	HTAIARYSWWLFSTICMIVVLYFLATSLRSAAKE	: 172
HaCR1	: IYWARYSDWLFTTPPLLYDGLLAGADRNTITSLSVSLDVLMIGTGLVATLSPG--	SGVLSAGAERLVWWGISTAFLLVLYFLFSSLSGRVAD	: 166
CrChR1	: TVWLRYAEWLLTCPVILIHLSNLGLANDYNKRTMGLLVSDIGTIVWGTAAALSKGYVRVIFFLMLCYGIYTFNAAKVYIEAYHTVPKGIV		: 245
CrChR2	: VQWLRYAEWLLTCPVILIHLSNLGLSNDYSRRTMGLLVSDIGTIVWGATSAMATGYVKVIFFCLGLCYGANTFFHAAKAYIEGYHTVPKGIV		: 206
PsChR2	: TPWLRYAEWLLTCPVILIHLSNITGLNDDSGRTMSLITSGLGGICMAVTSALSKGWLFFVIGCCYGASTFYHAALTYIESYYTMPHGV		: 189
MvChR1	: SPQLRYMEWLMTCPVILIAISNITGMAEEYNKRTMLLTDVCCIVLGMMMSAASKPRLKGILYAVGWAEGAWTYWTALQVYRDAHKAVPKP--		: 224

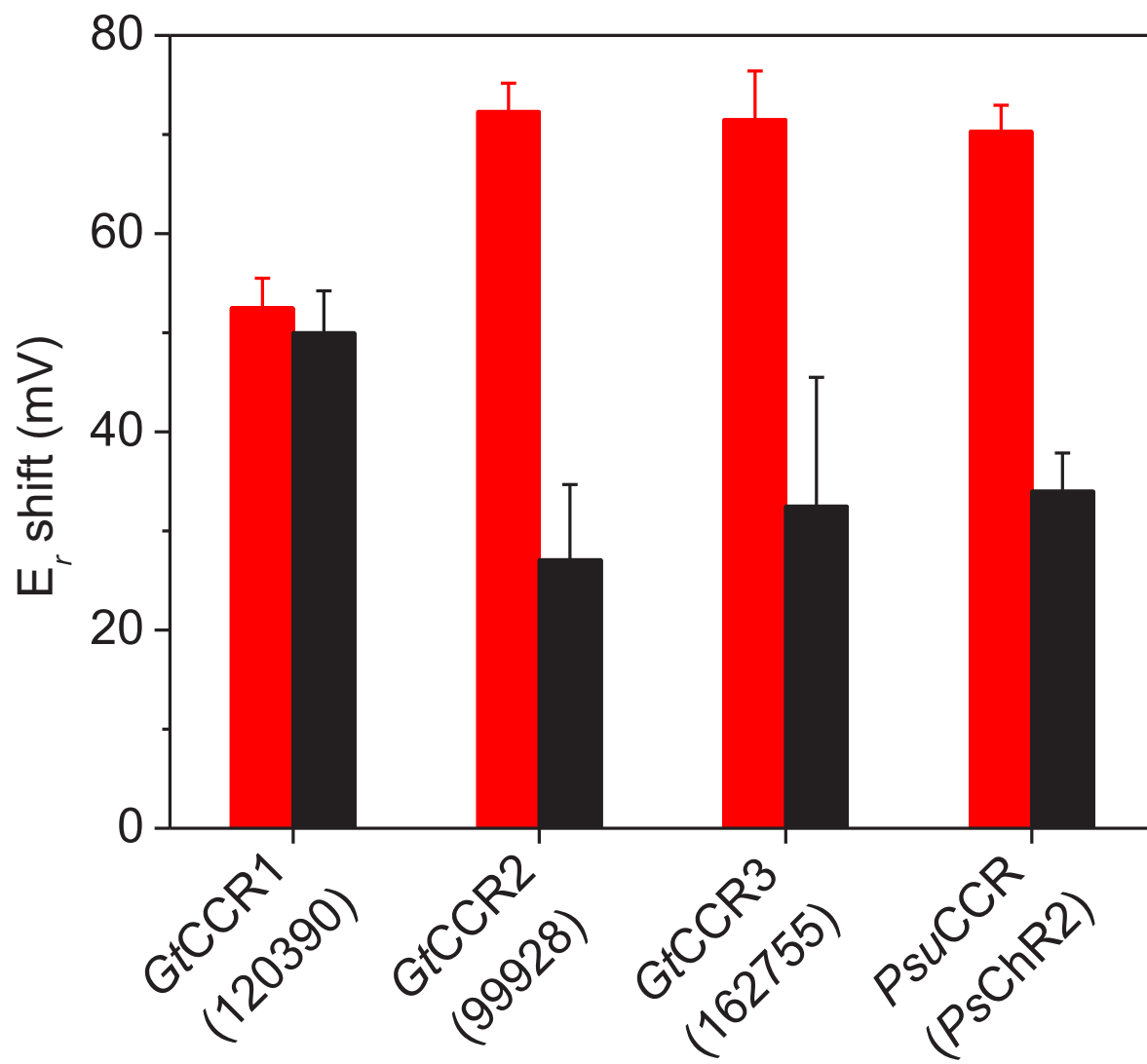
helix 6**helix 7**

GtCCR1	: SNAKRSIKHLKAAVIIYFGIWPPIFAILWLLSYRAANVILSNDTNHILHCILDVIAKSCFGFVLLHFKMYFDKKLLESG	: 245
GtCCR2	: SNAKQSLKHLKTAVFIFYFGIWLFLWLISYRAANVILSNDINHIFHCILDVIAKSVYGFALLYFKMYFDKKLIESG	: 245
GtCCR3	: ---KKVQSLKVACMTYFFIWLGYPTLWVLGDAG--VLDSSVVSALLHTFLDVFSKSIYGFALLHFVMTDKREFIFV	: 251
PsuCCR	: TKAEGALFSLKLAIITFFAIWVAFPLVWLLSVG TG-VLSNEAAEICHCHCICDVVAKS VYGFALANFREQYDRELYGILL	: 271
HsBR	: M-RPEVASTFKVLRNVTVVLWSAYPVVWLIGSEGAGIVPLNIETLLFMVL DVSAKVGFLILLRSRAIFGEAEAPEP	: 238
HspAR2	: R-SEEVRSTFNTLTALVAVLWTAYPILWIVGTEGAGVVG GLIETL AFMVL DV TAKVGFGFVLLRSRAILGETE APEP	: 249
HsoAR3	: R-GPEVASTFNTLTALVVLWTAYPILWIIIGTEGAGVVG GLIETL FMVL DV TAKVGFGFILLRSRAILGDTE APEP	: 248
HaCR1	: L-PSDTRSTFKTLRNLTVVWLVYPVWWLIGTEGIGLVGIGIETAGFMVIDITAKVGFGIILLRSRGVLDGAETTG	: 242
CrChR1	: -----CRDLVRYLAWLYFCSWAMPFPVLFLLGPEGFGHIINQNSAIAHAILDIASKNAWSMMGHFLRVKIHEHILLYG	: 318
CrChR2	: -----CRQVVTGMAWLFFVSWGMFPILFILGPEGFGVLSVYGSTVGHIDIIMSKNCWGLLGHYLRVLIHEHILHG	: 279
PsChR2	: -----CKNMVLAMA AVFFT SWMF PGFL FLAGPEGTNAL SWAGSTI GHTVADILSKNAWMIGHFLRLIEIHKIIIHG	: 262
MvChR1	: -----LAWYVRAMGYVFTSWLTFPGWFLLGPEGLEVVTGTVSTLMHACSDIISKNLWGFM DWHLRLVVARHHRKL	: 297

Supporting figure 2. A ClustalW partial protein alignment of four cryptophyte CCRs used in this study: *GtCCR1* aka 120390 (KU761994), *GtCCR2* aka 99928 (KU761992), *GtCCR3* aka 162755 (KU761993) and *PsuCCR* aka *PsChR2* (KF992056). For comparison are also included haloarchaeal proton pumps: *HsBR*, *Halobacterium salinarum* bacteriorhodopsin (V00474), *Halobacterium* sp aus-2 archaeorhodopsin-2 (S56354), *Halorubrum sodomense* archaeorhodopsin-3 (GU045593), *Haloarcula argentinus* cruxrhodopsin-1 (D31880), and chlorophyte CCRs: *Chlamydomonas reinhardtii* ChR1 (AF508965), *Chlamydomonas reinhardtii* ChR2 (AF508966), *Platymonas (Tetraselmis) subcordiformis* ChR2 (JX983143), and *Mesostigma viride* ChR1 (JF922293). Numbers in parentheses are GenBank accession numbers. Amino acid residue numbering and helical regions are according to the *HsBR* sequence. The Glu residues conserved in helix 2 of chlorophyte CCRs but not found in cryptophyte CCRs or haloarchaeal rhodopsin proton pumps are highlighted green, and the Asp residues conserved in helix 3 of haloarchaeal rhodopsin proton pumps and cryptophyte CCRs are highlighted red.



Supporting figure 3. The mean amplitudes of stationary photocurrents (red bars, left axis) generated by cryptophyte CCRs in HEK293 cells at the saturating light intensity and the wavelengths of the maximal sensitivity for each protein (see Fig. 2 in the main text), and half-decay rates of these currents upon switching off the light (black bars, right axis). The data are the mean values \pm SEM ($n = 5\text{-}14$ cells). Although the current amplitudes also reflect expression levels, expression yield was not the reason for the observed differences, because the intensities of the tag fluorescence of all tested constructs were similar. The half-decay rate of the current decay (half-closing of the channel) is the reciprocal of the time when the stationary photocurrent amplitude decreases 50% after switching off the light.



Supporting figure 4. The shifts of E_r upon a 100-fold reduction of the Na^+ (from 150 mM to 1.5 mM; red bars) or H^+ (from pH 5.4 to pH 7.4; black bars) concentration in the bath determined for cryptophyte CCRs by measuring the IE curves as shown in Fig. 3 c in the main text. The data points are the mean values \pm SEM ($n = 3\text{-}5$ cells).

Supporting References

1. Huson, D. H., C. Scornavacca. 2012. Dendroscope 3: an interactive tool for rooted phylogenetic trees and networks. *Syst. Biol.* 61:1061-1067.
2. Zhang, H., S. Gao, ..., W. H. Chen. 2012. EvolView, an online tool for visualizing, annotating and managing phylogenetic trees. *Nucleic Acids Res.* 40:W569-572.